

Tracking electron capture processes in classical molecular dynamics simulations for spectral line broadening in plasmas

D. González-Herrero,¹ G. Pérez-Callejo,¹ R. Florido,² and M. A. Gigosos^{1,*}

¹*Departamento de Física Teórica Atómica y Óptica, Universidad de Valladolid, 47011 Valladolid, Spain*

²*iUNAT-Departamento de Física, Universidad de Las Palmas de Gran Canaria, 35017 Las Palmas de Gran Canaria, Spain.*

(Dated: February 10, 2025)

Plasma spectroscopy is a fundamental tool for diagnosing laboratory and astrophysical plasmas. Accurate interpretation of spectra depends upon precise modeling and comprehension of Stark-broadening and other mechanisms affecting spectral lines. In this context, computer simulations have emerged as invaluable tools, offering *idealized experiments* with well-defined conditions. Molecular dynamics simulations, in particular, excel at replicating the particle interactions within the plasma and their impact on the state of a radiating atom or ion. However, these simulations present challenges in tracking electron capture processes, since setting an unambiguous criterion to distinguish between bound and free electrons is not trivial. In this paper we introduce a new algorithm that, within a classical framework, precisely identifies the scenario in which an electron is captured by an ion and then follows a stable orbit around it. The algorithm's applicability extends to emitters with charges $Z \geq 1$. Importantly, the procedure enables the correct identification of valid time-histories of the electric microfield perturbing the emitting ion, which will be used for subsequent line shape calculations. As a result, our simulations naturally and accurately incorporate the effects of both strong collisions and electron capture phenomena on spectral line broadening.

I. INTRODUCTION

Accurate modeling of spectral line shapes is indispensable for investigating the properties of high energy density plasmas. The analysis of emission or absorption spectra, which typically involves the comparison of experimental data with spectroscopic models, stands as a key diagnosis tool for laboratory and astrophysical plasmas. Spectral line shapes, broadened and shifted by the kinetics of plasma particles and their interactions, provide relevant information about the plasma temperature and density; and play a pivotal role in opacity calculations, crucial for radiation hydrodynamics simulations.

Spectral lines arise from atomic transitions between bound energy states of the radiator. In the context of hot and dense plasmas the Stark effect emerges as the dominant broadening mechanism [1]. Unlike the isolated scenario, when embedded in a plasma, the radiator is subject to the electric field generated by its surrounding charged particles during the radiation time interval. The shape of the spectral lines in this case depends on the plasma-induced electric field, its time evolution (tied to the the plasma particle dynamics) and the radiators' ensemble.

Despite significant strides in recent decades [2, 3], modeling spectral line shapes remains a formidable challenge owing to its interdisciplinary nature, requiring the integration of various ingredients from atomic physics, plasma physics, statistical mechanics, collision theory, and computational physics. Moreover, in the high-density regime, dedicated validating experiments are notably scarce, presenting a substantial obstacle to ground-

ing theoretical models in empirical reality. In response to these challenges, the Spectral Line Shapes in Plasmas workshop series [4–7] has emerged as a valuable initiative, providing a platform to compare the multiple approaches to the problem, identify sources of discrepancies, and scrutinize the validity of different approximations. Such collaborative endeavors have stimulated the specialized community to undertake a deeper exploration of missing physics in line broadening theory and to improve the reliability of the existing models.

Two primary approaches are used for line-broadening calculations: analytic methods and computer simulations. Analytic models navigate the complexities of line broadening by incorporating assumptions and mathematical manipulations to handle the stochastic nature of line emission. One common approximation involves the separate calculation of electron and ion broadening contributions. Since ions are much heavier than electrons, they are assumed to be static over the relevant electron time scales. The analytic approach then puts the effort in obtaining an accurate representation of the electron broadening operator. In this regard, some common approximations include the simple and well-known *impact* approximation, or the *second-order* approximation as a simplified way to compute the electron broadening operator. Once the electron broadening contribution is computed for a given ion distribution, i.e. for a given value of the ion microfield, the line emission is integrated over the statistical distribution of the ion microfield for the conditions of interest, a facet that entails its own extensive research area in microfield probability distributions. The inherent advantages of analytic methods lie in their computational efficiency, as the time required to calculate a line shape is generally much shorter than for computer simulations, and they operate without numerical noise.

On the other hand, simulations prove particularly ad-

* gigosos@coyanza.opt.cie.uva.es

vantageous in gaining insights into the line broadening problem, excelling at replicating plasma particle interactions and their impact on the state of a radiating atom or ion. Simulated plasma particles traverse within a confined space, following classical trajectories. These classical particles generate a time-dependent Coulomb potential or, equivalently, a time-sequence of the electric field, which is then utilized to solve for the time evolution of the radiator, subsequently generating a spectrum. Simulations often simplify the problem and reduce computational time by employing straight-line paths or hyperbolic trajectories for particle movement. Noteworthy exceptions to this norm are molecular dynamics simulations, such as the ones presented in this work, which uniquely account for full N-body interactions.

It is in this context that our work is framed. We present an algorithm to accurately track the electron capture processes within molecular dynamics computer simulations, key to obtain the correct time-sequences of the electric field within the plasma and accurately account for the additional recombination broadening.

This manuscript is structured as follows: in Section II, we give an overview of how computer simulations in the context of line broadening calculations work and present the need for an algorithm capable of detecting electron capture process. Section III details the criterion itself. An example of the application of this criterion to a computer simulation is presented in Sec. IV A, and a comparison of our results with an additional ionization metric is given in Sec. IV B. Finally, Sec. V summarizes the conclusions and limitations of this work.

II. OVERVIEW OF COMPUTER SIMULATIONS

Computer simulations for calculating Stark-affected spectra usually follow these steps [8]:

- a) In a computer, one reproduces a plasma composed of charged and/or neutral particles which are distributed in a given region of space. These particles move according to certain pre-established statistical distributions which arise from a given physical configuration (electron density and temperature). The simulation evolves in discrete timesteps and the calculation permits the description of the position and velocity of the particles at every timestep.
- b) The simulated plasma includes the emitters that are considered for the spectral calculations. For each timestep, the electric field produced by all plasma particles on a given emitter is calculated. This is the time-dependent field sequence that this work focuses on.
- c) The emitting atom or ion internally evolves, subjected to the effect of this electric field. By numerically solving the time-dependent Schrödinger equation, one obtains the corresponding evolution

operator. It is then possible to calculate the dipolar moment of said emitter as a function of time. The Fourier transform of the autocorrelation function of this dipolar moment corresponds to the emission spectrum from the emitter under consideration.

- d) This process is repeated a sufficient number of times. The average value of the individually produced spectra corresponds to the spectrum of interest.

Let us now consider exclusively the first step of the process described above: the numerical treatment of the simulated plasma. Generally, we can consider two types of computer simulations: those where the particles are considered physically and statistically independent, and those which take into account the interactions among charged particles. In the first case, the idea is to numerically reproduce a plasma of free and independent particles that move within the plasma following rectilinear trajectories with fixed velocities. We will refer to these methods as Trivial Molecular Dynamics (TMD). In the second case, the calculation takes into account the electric interaction of all particles in the plasma. It is a more accurate method (and more computationally expensive) which must solve Newton's equations of motion to determine the trajectories of all particles. We will refer to these methods as Full Molecular Dynamics (FMD).

TMD calculations, much more computationally affordable, are useful when the typical electric-interaction energies are much lower than the mean kinetic energy of particles (a weakly-coupled high temperature plasma) and, specially for non-charged emitters [9–14]. The second method (FMD) is necessary for medium and strongly-coupled plasmas and, specially when the emitter is an ion, given that its interaction with the surrounding particles in the plasma affects both its own trajectory and those of the other particles, thus modifying the time-evolution of the electric field of interest [15–17]. In this work, we focus on this type of calculations.

It is worth mentioning that there is an intermediate type of calculations, in which the perturbers are treated as independent particles, but their interaction with the emitter is taken into account explicitly. This results in the charged perturbers moving in hyperbolic trajectories when a Coulomb field is considered, or in slightly different paths if Debye screening is introduced, in which case the corresponding differential equation must be solved numerically [18].

In a FMD simulation, the Coulombian interaction between the plasma particles is considered classically. To avoid divergencies in the electron-ion interaction energies at short distances, it is necessary to *regularize* the interaction potential. Several procedures for this regularization have been reported (see Bonitz *et al.* [19] and references therein), and in this work we will use that described in Gigosos *et al.* [20], which considers a parabolic potential for interparticle distances below a given value a and hyperbolic for larger distances. This procedure nat-

usually accounts for the diffraction of electrons around an ion and determines an effective atom size.

During the evolution of the simulation, it is possible that the binding energy (negative) between an electron and an ion becomes too large - in absolute value - with respect to their kinetic energies, so that the electron becomes *trapped* by the ion. In that case, the electron becomes bound and its trajectory follows an orbit around the ion. The two particles in this pair can therefore no longer be considered free and must be labeled as a neutral atom, or as an ion with a positive charge lower than that of the free ion. This circumstance has been extensively discussed in our previous work [20], where we developed a statistical model for the equilibrium of the simulated plasma, taking into account the process of electron capture and release by the ions (recombination and ionization respectively). The model perfectly reproduces what is observed in the simulation, therefore allowing us to correctly determine the density of free electrons in the plasma, considering that these *trapped* electrons do not contribute to its value. For this model, it was necessary to establish a clear criterion to determine when an electron-ion pair must be considered bound, and when those particles must be considered free. While in Gigosos *et al.* [20] ions of charge $+q_e$ were used (where q_e is the electron charge), in this work we are interested in plasmas with charge $+Zq_e$, with $Z > 1$. The purpose of this work is then to extend this criterion to situations in which the number of trapped electrons can exceed 1.

The need for such a criterion is obvious. In the simulations, it is necessary that the density of free electrons is a given value (generally predetermined). To calculate such value, one needs to *count* the electrons that are really free in the simulated plasma. This number does not match that of the electrons included in the calculations, since some of them will become bound to the ions.

Furthermore, there is another important reason that requires knowing when an ion has captured an electron and when it can be considered free. Let us consider a FMD simulation in which we are interested in calculating the spectrum from an ionic emitter with charge $+Zq_e$. To that end, during the simulation process, we must register the temporal sequence of the electric field *seen* by that charged emitter, which is produced by the ions and free electrons surrounding it. If, at a given moment, an electron is captured by the ion of consideration, from that moment on, the electron will orbit around it at a short distance. Therefore, the electric field felt by that emitter will be an oscillating function with a large amplitude (since the oscillating electron is very close), which spoils the field sequence. In addition, this ion, originally with charge $+Zq_e$ has now become, along with the trapped electron, an ion of charge $+(Z-1)q_e$ and can therefore no longer be considered a contributor to the spectral line in which we are interested. The moment the electron is captured determines when the ion changes its *species* and therefore completely breaks the coherence of the spectral line that was being emitted. This problem was already

considered in Gigosos *et al.* [17], where the process is discussed but no details are given on the criterion that the computer follows to determine when an electron can be considered bound or truly free. This is the purpose of this work.

III. CRITERION FOR DETECTING TRAPPED ELECTRONS IN A COMPUTER SIMULATION

As mentioned before, *detecting* ionization and recombination processes is of fundamental importance in computer simulations. In these calculations, when the ion whose spectrum is being calculated captures an electron, it no longer belongs to the ion species of interest and, therefore, its internal evolution is not relevant: the emission coherence is abruptly lost. This causes a broadening of the line by the recombination process, which highlights one the advantages of these calculations [17]. As a consequence, in practice, the corresponding time-sequence of the electric field is *cut* in the simulation process. It is necessary then to wait for the corresponding ion to recover its original charge in order to continue using it for the calculation.

Usually, electrons are labeled as *bound* to an ion when their distance is lower than a given value r_{min} (whose value is discussed in Gigosos *et al.* [20]) and the total energy (kinetic plus potential) of the electron-ion pair is negative. While this criterion [21] works well in most cases, it gives some wrong answers. Moreover, for ions with charge $Z > 1$, this method only detects if an ion has some electron trapped, but not how many [22].

If one follows this criterion, it is possible for an electron to orbit at distances larger than r_{min} (and thus be considered *free*), but still produce a non-physical oscillating electric field on the ion. On the other hand, for strong enough collisions (an electron gets closer than r_{min} to an ion, but only momentarily), the total energy of the electron-ion pair can become negative, which, following this criterion, would be wrongly considered as them being *bound*. Since these collisions happen regularly, this criterion effectively eliminates long field sequences of the Stark calculation, as they are broken every time a false bound pair is detected. Furthermore, under this criterion, the field sequences considered will underestimate the effect of strong collisions. These two effects become more important for ions with charge $Z > 1$ (as more electrons can become bound), and more strongly coupled plasmas.

To correctly select the valid field sequences we choose a global criterion, in which whether an ion has trapped an electron or not, not only depends on its conditions at a given time, but also on its history. For a given ion, we store (for each step of the simulation) its potential energy, the electric field at its position and the *label* (an index identifying each electron in the simulation) of the $Z+1$ closest electrons, where Zq_e is the charge of the emitter. For this work, we rescaled the ion-electron po-

tential energy defined in Gigosos *et al.* [20] for $Z = 1$ ions, to

$$V_{ie}(r) = \begin{cases} V_i \left[\frac{1}{3} \left(\frac{r}{a} \right)^2 - 1 \right], & r \leq a \\ -\frac{Zq_e^2}{4\pi\epsilon_0} \frac{1}{r}, & a < r \leq R_I \\ 0, & r > R_I \end{cases} \quad (1)$$

where V_i is the ionization energy corresponding to the ion of charge Z and R_I is the radius of the interaction sphere, defined as half the size of the cubic simulation box. For ions with $Z > 1$, a is also rescaled as

$$a = \frac{3}{2} \frac{Zq_e^2}{4\pi\epsilon} \frac{1}{V_i}. \quad (2)$$

The first step then is to track down the moments when the potential energy of the emitter is lower than a given value. In particular, we chose a threshold energy of

$$\mathcal{E}_{th} = -\frac{3}{4}V_i. \quad (3)$$

Whenever the ion energy is lower than \mathcal{E}_{th} , the electron that is closest to it (its first neighbor) is identified. Then, the time interval during which that electron has been among the $Z + 1$ closest neighbors is considered. If this interval is longer than a given threshold value, then the average total energy of the electron-ion pair in that interval is calculated. If the pair has a negative total energy during that interval, then the electron is considered to be bound for the whole interval. If not, it is considered that the negative energy seen by the emitter is caused by a strong collision, since the electron causing it did not remain around the ion. It is worth noting that the $Z + 1$ closest neighbors are considered, since it is possible that a fast electron gets closer to the ion core than other bound electrons for a short period of time, without freeing them.

Since the full time-history of the ion is needed in order to check whether an electron is bound or free, its history must be saved to files in the disk. In this way, it can be accessed when the energy criterion is met, and the correct field sequences can be extracted.

Determining the timescale of bound electrons in the simulation

In the classical picture of these FMD simulations, an electron orbiting an ion will do so with a given period, such that the orbit is stable. For a hyperbolic potential (such as the Coulomb potential), the condition for a stable orbit is given by

$$m_e v^2 = \frac{Zq_e^2}{4\pi\epsilon_0 r}, \quad (4)$$

where m_e is the electron mass, v its velocity, and r the orbit radius. Under this condition, an electron orbiting an

ion at the typical thermal velocity ($v_T = \sqrt{2k_B T_e/m_e}$, with k_B the Boltzmann constant and T_e the electron temperature) will do so at a distance of

$$r_T = \frac{Zq_e^2}{8\pi\epsilon_0 k_B T_e}, \quad (5)$$

and therefore, the corresponding orbital period is given by

$$\tau_T = \frac{2\pi r_T}{v_T} = \frac{Zq_e^2}{2\epsilon_0} \cdot \frac{m_e^{1/2}}{(2k_B T_e)^{3/2}}, \quad (6)$$

or, in simulation units¹

$$\tau_T^{S.U.} = \frac{\pi}{3} Z \rho^2 \quad (7)$$

We take this characteristic orbit time as a basis to consider whether an electron is bound to an ion. Although one might be tempted to consider τ_T as the temporal threshold - that is, if an electron is within the $Z + 1$ closest neighbors of a given ion for at least τ_T , and its total energy is negative, it is considered bound - this criterion would overestimate the number of bound electrons, since an electron can loop around an ion once without being bound. For this reason, we choose $\tau_{th} = 3\tau_T$ as the threshold for considering an electron as bound to a given ion.

We note here that the above expression for τ_T was obtained for a hyperbolic potential. However, as indicated in Eqn. 1, in our simulations, the potential becomes parabolic for distances $r < a$, and thus, care must be taken to ensure that $r_T > a$. By comparing the above expressions for both r_T and a , it can easily be seen that this condition is equivalent to

$$\frac{V_i}{2} > \frac{3}{2} k_B T_e. \quad (8)$$

Therefore, the criterion is valid if the ionization potential is larger than twice the thermal energy of electrons. However, this is always the case when recombination effects are relevant given that, in reality, if the temperature is high enough so that it becomes comparable with the ionization potential, the electrons are all free, and recombination effects are negligible (as we will show in the following section).

¹ The units that the simulation works with are important. The relation between the numbers in the simulation and physical magnitudes is determined by two parameters in the simulation: (1) the coupling degree ρ , which is a non-dimensional parameter whose value is fixed prior to the simulation and corresponds to the relation between the typical distance between electrons and the Debye radius; and (2) the value of the ionization potential in simulation units (which is also fixed). The unit of length is taken as the typical distance between electrons (free or not), the unit of time is the characteristic time in the electron dynamics, and the unit of mass is that of the electron. In this manuscript, we work with those units. \mathcal{E}_0 is the corresponding unit of energy, and E_0 that of the electric field. For a more detailed discussion on the units in the simulation, see Gigosos *et al.* [20].

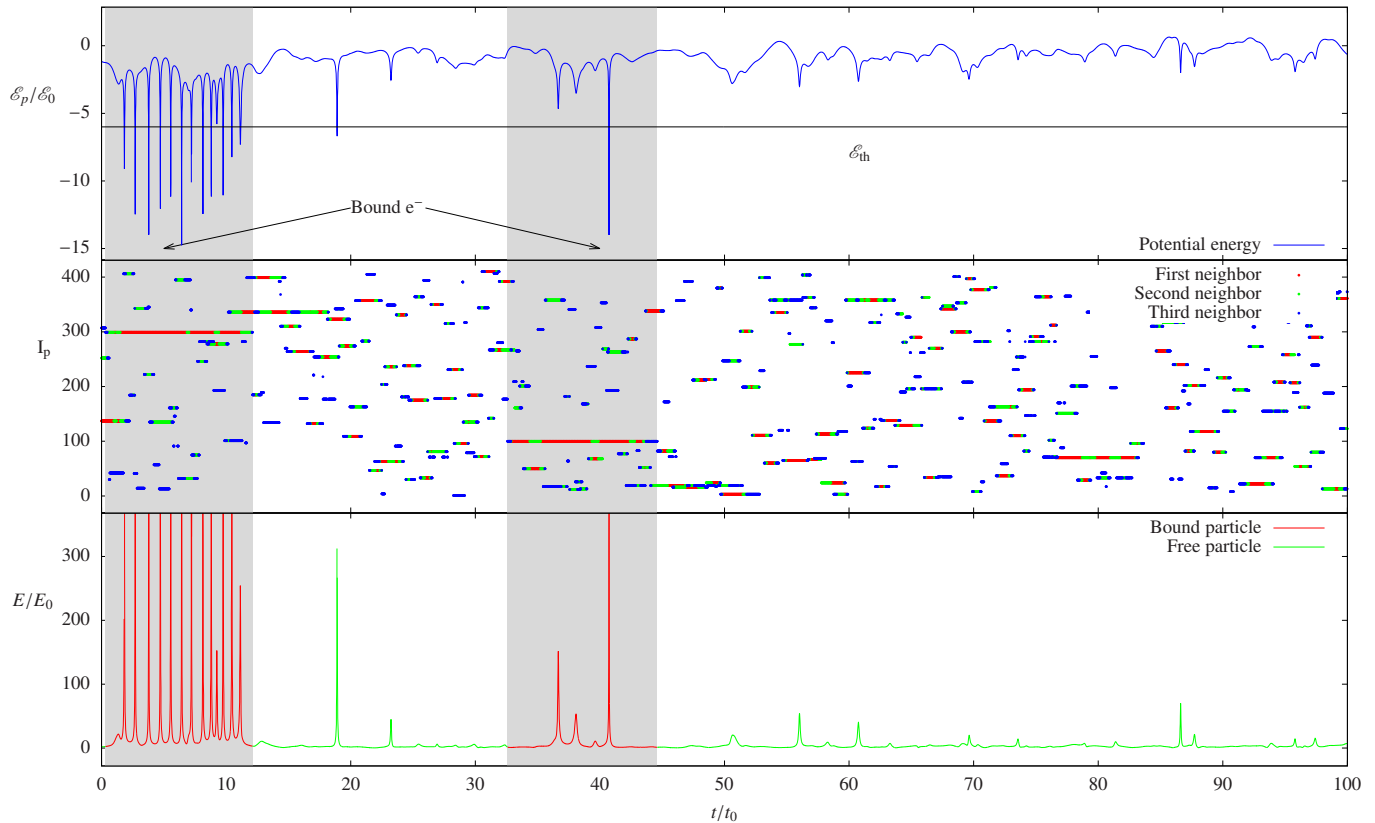


FIG. 1. Time-history of a plasma with $\rho = 0.6$ and emitters with charge 2. From top to bottom: potential energy of an emitter as a function of time, indices of the three closest electrons at each moment, and electric field. The shaded regions correspond to the moments when a particle is trapped (see footnote 1).

IV. RESULTS AND DISCUSSION

A. Application of the criterion

Let us now show an example of the application of this method, for the particular case of ions with charge $Z = 2$, which means that the three closest neighbors must be monitored. In this example, the coupling parameter of the plasma is $\rho = 0.6$, and therefore $\tau_T \sim 0.75$ in simulation units. Figure 1 shows the time-history of the potential energy of an emitter (top), the indices I_p of the three electrons that are closest to it at every timestep in the simulation (middle) and the value of the electric field acting on said emitter (bottom panel). At $t \sim 2t_0$ (with t_0 being the time unit in the simulation), when the potential energy becomes lower than \mathcal{E}_{th} , the electron that is closest to the emitting ion is electron number 298. We then observe that this electron has been among the three closest neighbors from $t \sim 0$ to $t \sim 10t_0$, approximately 10 times the characteristic time of the simulation. This is much longer than the typical duration of a collision, so we must assume that this corresponds to a bound electron. Indeed, if we now consider the electric field between

$t \sim 0$ and $t \sim 10t_0$, it oscillates periodically - with a period of approximately $0.75t_0$, which is the value of τ_T in this case - with very high values. A similar situation is observed at $t \sim 35t_0$, although in this case the trapped electron oscillates around the ion only a few times, and therefore its imprint on the electric field history is not as clear.

It can be seen that this system does not eliminate strong collisions, as discussed above. For example, at $t \sim 20t_0$, the potential energy jumps below the threshold value, as an electron passes very close to the emitting ion. However, the colliding electron does not remain among the three closest neighbors for long enough to be a bound particle. Indeed, the electric field history confirms that this corresponds to an isolated collision.

B. Validation of the trapped-electron detection algorithm: calculation of the ionization balance

So far we have described the algorithm that allows tracking the electron trajectories in time and eventually determine whether a particular one has been trapped by an ion or not. Accordingly, this procedure allows identi-

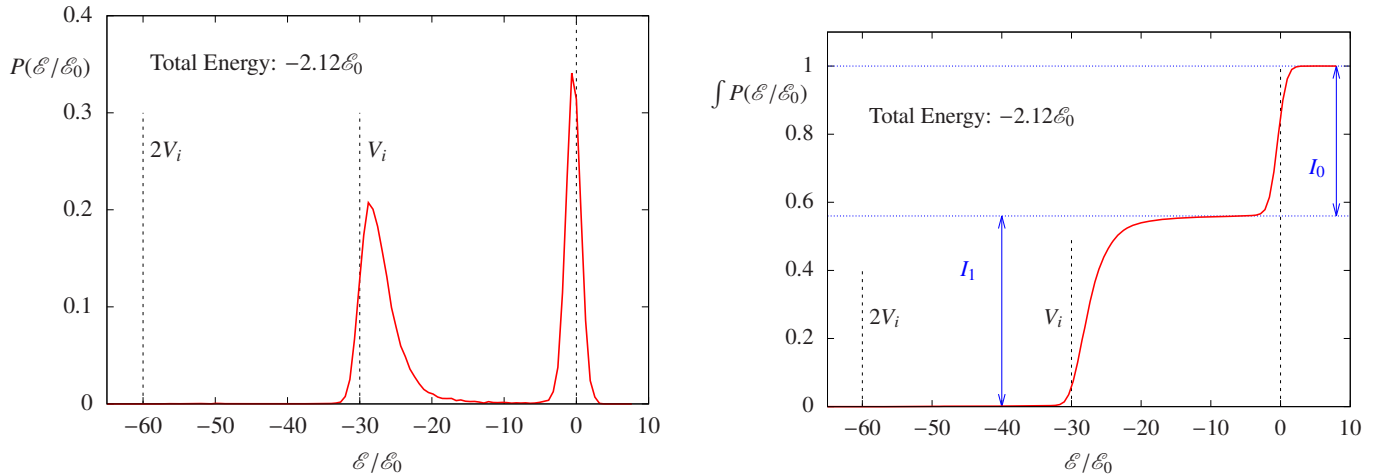


FIG. 2. Distribution of the potential energy of the ions (left) and its integral (right). Data correspond to a Helium plasma ($Z = 2$), with an ionization potential $V_i = 30 \mathcal{E}_0$, and a nominal coupling parameter $\rho_N = 1.0$. The mean total energy per particle of the system is $\mathcal{E}_i = -2.12 \mathcal{E}_0$.

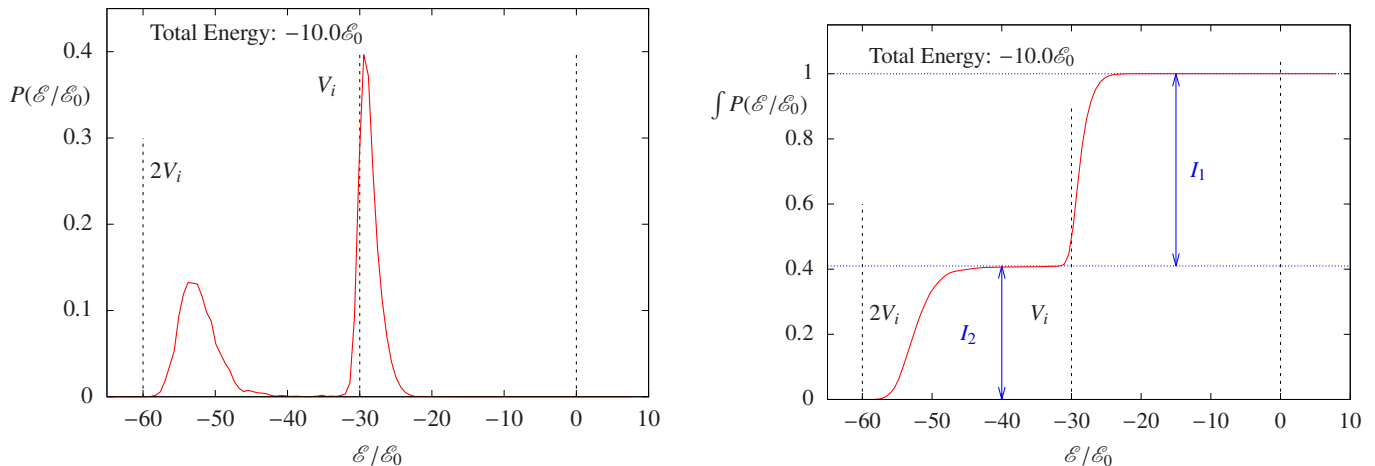


FIG. 3. Same as in Fig. 2, with a mean total energy for particle of $-10.0 \mathcal{E}_0$.

fyng and storing the appropriate electric field sequences that will be further used for line shape calculations.

It would be convenient to validate the trapped-electrons detection algorithm using a different independent method, also arisen and consistent with the FMD framework. In this regard, we note that by applying the trapped electron detection algorithm one can easily determine the fractional population of different ion charge states in the plasma at given conditions and therefore obtain the corresponding ionization balance.

It turns out that the plasma ionization balance can also be obtained from the analysis of the ion potential energy distribution. Once the equilibration time is achieved for a particular simulation run, one can now take a sufficiently large number of simulation snapshots during the

equilibrium stage, compute the potential energy distribution for each of them and finally take the average in order to get a good statistical representation (smooth) of the potential energy distribution of the plasma particles at given conditions. To ensure proper statistics, additionally we take the average over a collection of simulation runs (~ 10) starting with different initial conditions always consistent with the plasma conditions of interest. As explained below, the plasma ionization balance can be inferred by properly interpreting the potential energy distribution. We note that this is a robust method that does not require the definition of ad-hoc criteria to label an electron as bound or free. On the contrary, due to its own statistical nature, this method is not useful for selection of electric field sequences since the time-resolved

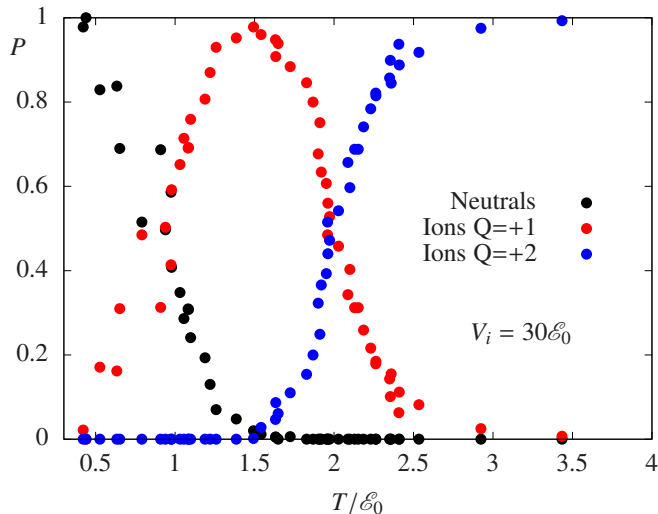


FIG. 4. Fractional population of the different ion species as a function of the temperature for a plasma of ions with charge 2, and an ionization potential of $V_i = 30\epsilon_0$. Each dot corresponds to a set of simulations with the same temperature at equilibrium.

information is lost. Hence, the comparison of the ionization balance obtained from the trapped-electron detection algorithm against the one from the analysis of the potential energy distribution provides a way to validate the former, adding confidence on the selected electric field sequences for line shape calculations.

For illustration let us first assume the simple case of hydrogen ions ($Z = 1$). If the plasma temperature is low enough (in simulation units) so that the distribution of kinetic energies is relatively narrow, the distribution of potential energies presents two main lobes. One of them centered around zero (free particles), and one of them near the potential well of energy V_i (ions with a bound electron) - see figure 14 in Gigosos *et al.* [20] -. Following this logic, it can be easily seen how for ions with $Z = 2$, the distribution of potential energies can have up to three lobes: that corresponding to free particles, around zero potential energy; the one accounting for ions with one bound electron, with potential energies similar to V_i ; and the lobe corresponding to ions with two trapped electrons, which will have energies similar to $2V_i$. If these three groups are sufficiently separated, it is possible to integrate the energy distribution and associate the area under each lobe to the population of the different species.

This is illustrated in Figure 2, in which we show the distribution of potential energies (left) and its integral (right) for an equilibrated plasma of $Z = 2$. The corresponding potential well is $V_i = -30\epsilon_0$, and the mean total energy per particle is $-2.12\epsilon_0$. The distribution of potential energies therefore only presents two lobes, centered around zero and V_i . In this case, the energy per particle is relatively high compared with the ionization potential, and therefore only two ionization species

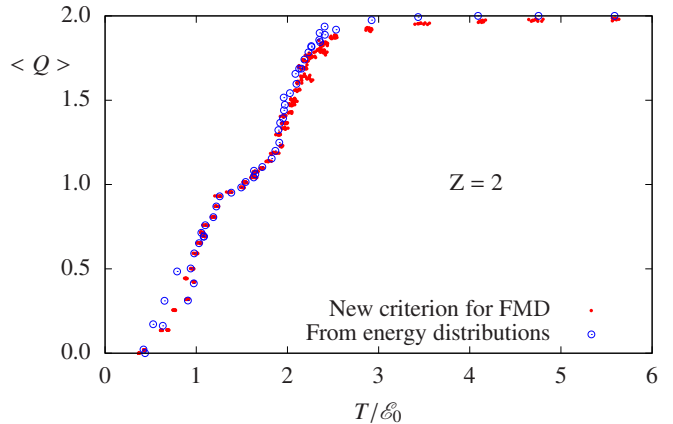


FIG. 5. Mean ion charge obtained by applying the new criterion for selecting electric field sequences, compared to the values obtained by integrating the potential energy distributions. It can be seen that the results are in very good agreement.

are present in the plasma: free ions and those with one bound electron. By looking at the integral of the energy distribution (plot on the right), the ratio of ions with one bound electron (I_1) to free particles (I_0) can be easily obtained.

A similar example is shown in Figure 3 for the case when the plasma mean energy is $-10\epsilon_0$. The rest of the plasma parameters are identical as those in Fig. 2. In this case, the plasma energy is too low, and the plasma is composed of only ions with one (I_1) or two bound electrons (I_2), with almost no free ions.

Using this method, we calculated the fractional population distribution for a collection of simulation runs spanning over a wide range of plasma temperatures. The results are shown in Figure 4, where the different colors correspond to the population fraction of the different ion species as a function of temperature. We note that each dot in fact corresponds to a group of different simulations associated to the same temperature value, i.e. for a given temperature, a number of simulations starting from different initial conditions were launched and then let to thermalize following the method described in our previous work [20]. As expected, at low temperatures all ions have two bound electrons and, as the temperature increases, some electrons become free, leading to an increase in the population of ions with only one bound electron. The number of ions with $Q = +1$ keeps growing until almost no neutral ions remain. If the temperature is increased further, ions can become doubly ionized ($Q = +2$), until there are no more bound electron-ion pairs.

Once the ion population distribution is calculated, one can easily obtain the average ionization. We show this in Figure 5, together with the results obtained from the application of the trapped-electron detection algorithm for the same temperature range. The agreement between

the two methods is remarkable, which firmly constitutes a validity proof of the detection algorithm. Furthermore, as mentioned in the previous section, it can be seen that, even when the temperature becomes one tenth of the ionization potential, most atoms are fully ionized, and recombination effects become negligible.

V. CONCLUSIONS

In this study, we have introduced a robust criterion for tracking and identifying trapped electrons within *Full Molecular Dynamics* (FMD), specifically focusing on ions with charges $Z > 1$. Our presented criterion effectively distinguishes strong collisions within the plasma from recombination effects, providing a clear understanding of the underlying processes. Moreover, this method offers a pathway to determine the plasma ionization balance under specific conditions.

To validate our detection algorithm, we conducted extensive comparisons across a wide range of plasma temperatures. Specifically, we compared the average ionization values obtained through our criterion with those derived from a well-established method based on the analysis of ion potential energy distribution. It is important to note that while our ionization balance calculations do not claim to precisely solve plasma atomic kinetics, our full molecular dynamics simulations accurately capture the plasma ionization balance within the framework of the classical ionization-recombination mechanism. It is worth mentioning that this classical approach lacks a distinct quantum-mechanical counterpart.

Our simulations, though comprehensive, do not encompass dissipative radiative processes. Consequently, the classical recombination mechanism incorporated in our simulations cannot fully account for radiative recom-

ination; rather, it represents a combined effect arising from electron capture and likely three-body recombination. Nevertheless, the detection algorithm discussed in this study serves as a valuable tool for tracking the ionization-recombination mechanism within full molecular dynamics simulations involving ions with $Z > 1$. This inclusion is pivotal, especially when considering the additional recombination width on spectral line shapes.

Importantly, without a methodology akin to the one presented in this study, such effects would be entirely overlooked, leading to inaccurate calculations of line profiles, particularly in strongly-coupled plasmas. By incorporating our detection algorithm, researchers can achieve more precise and reliable simulations, essential for advancing our understanding of spectral line broadening in complex plasma environments.

ACKNOWLEDGEMENTS

This work has been supported by Research Grants No. ENE2015-67581-R/FTN (MINECO/FEDER-UE) from the Spanish Ministry of Economy and Competitiveness and PID2022-137632OB-I00 from the Spanish Ministry of Science and Innovation.

This work has also been carried out within the framework of the EUROfusion consortium, funded by the European Union via the Euratom Research and Training Program (Grant Agreement Nos. 633053 and 101052200—EUROfusion). The views and opinions expressed are, however, those of the author(s) only and do not necessarily reflect those of the European Union or the European Commission. Neither the European Union nor the European Commission can be held responsible for them. The involved teams have operated within the framework of the Enabling Research Projects: Grant number AWP21-ENR-IFE.01.CEA.

-
- [1] H. R. Griem, *Spectral Line Broadening by Plasmas* (Academic Press, New York, 1974).
 - [2] M. A. Gigosos, J. Phys. D: Appl. Phys. **47**, 343001 (2014).
 - [3] T. A. Gomez, T. Nagayama, P. B. Cho, D. P. Kilcrease, C. J. Fontes, and M. C. Zammit, Journal of Physics B: Atomic, Molecular and Optical Physics **55**, 034002 (2022).
 - [4] E. Stambulchik, High Energy Density Phys. **9**, 528 (2013).
 - [5] E. Stambulchik, A. Calisti, H.-K. Chung, and M. Á. González, Atoms **2**, 378 (2014).
 - [6] J. Rosato, High Energy Density Phys. **22**, 60 (2017).
 - [7] E. Stambulchik, A. Calisti, H.-K. Chung, and M. Á. González, Atoms **7**, 20 (2019).
 - [8] E. Stambulchik and Y. Maron, High Energy Density Phys. **6**, 9 (2010).
 - [9] R. Stamm and D. Voslamber, J. Quant. Spectrosc. Radiat. Transfer **22**, 599 (1979).
 - [10] M. A. Gigosos and V. Cardeñoso, J. Phys. B: At. Mol. Opt. Phys. **20**, 6005 (1987).
 - [11] G. C. Hegerfeldt and V. Kesting, Phys. Rev. A **37**, 1488 (1988).
 - [12] J. Rosato, Y. Marandet, H. Capes, S. Ferri, C. Mossé, L. Godbert-Mouret, M. Koubiti, and R. Stamm, Physical Review E **79**, 046408 (2009).
 - [13] M. Gigosos, S. Djurović, I. Savić, D. González-Herrero, Z. Mijatović, and R. Kobilarov, Astronomy & Astrophysics **561**, A135 (2014).
 - [14] T. Gomez, T. Nagayama, D. Kilcrease, M. Montgomery, and D. Winget, Physical Review A **94**, 022501 (2016).
 - [15] S. Ferri, A. Calisti, C. Mossé, B. Talin, M. A. Gigosos, and M. A. González, High Energy Density Phys. **3**, 81 (2007).
 - [16] E. Stambulchik, D. V. Fisher, Y. Maron, H. R. Griem, and S. Alexiou, High Energy Density Phys. **3**, 272 (2007).
 - [17] M. A. Gigosos, R. C. Mancini, J. M. Martín-González,

- and R. Florido, *Atoms* **9**, 9 (2021).
- [18] E. Stambulchik and Y. Maron, *J. Quant. Spectrosc. Radiat. Transfer* **99**, 730 (2006).
- [19] M. Bonitz, W. Ebeling, A. Filinov, W. Kraeft, R. Redmer, and G. Röpke, *Contributions to Plasma Physics* **63**, e202300029 (2023).
- [20] M. Gigosos, D. González-Herrero, N. Lara, R. Florido, A. Calisti, S. Ferri, and B. Talin, *Physical Review E* **98**, 033307 (2018).
- [21] N. Lara, *Calculations of Stark spectra of strongly coupled plasmas by molecular dynamics simulation*, Ph.D. thesis, University of Valladolid (Spain) (2013).
- [22] D. González-Herrero, *Study of the Stark broadening of the 3s-3p spectral lines in Be-like ions –Molecular Dynamics simulations–*, Ph.D. thesis, University of Valladolid (Spain) (2016).